Dynamics of a discrete population model for extinction and sustainability in ancient civilizations

Article *in* Nonlinear Dynamics Psychology and Life Sciences · February 2008

Source: PubMed

4 authors, including:


William Basener
University of Virginia


Bernard P. Brooks
Rochester Institute of Technology


Tamas Wiandt
Rochester Institute of Technology

DYNAMICS OF A DISCRETE POPULATION MODEL FOR EXTINCTION AND SUSTAINABILITY IN ANCIENT CIVILIZATIONS

BILL BASENER, BERNARD BROOKS, MICHAEL RADIN, AND TAMAS WIANDT

Abstract. We analyze a discrete version of a recently developed ratio dependent population-resource model. This model has been used to study the decline of the human and resource populations on Easter Island and the chaotic dynamics of moose and wolf populations in Canada. The dynamical system exhibits a rich behavior of fractal basins of attraction and a Neimark-Sacker bifurcation route to chaos. The model consists of a coupled pair of logistic equations, with the carrying capacity for the predators proportional to the number of prey.

1. Modelling Ancient Civilizations

Our goal in this paper is to analyze the dynamics of a population model for human populations with the possibility of a collapse, such as the population of Easter Island. Before discussing this particular model, which is given in Equation (4), we give an overview of long-term modelling of human populations and ancient civilizations.

Predicting human population dynamics over the long-term is a difficult endeavor which, historically, has been fraught with predictions which never came to pass. Individual people, with free will, are inherently unpredictable. Moreover, the continually changing factors of social norms and technological advances tend to thwart long-term predictions. In the late 1700's, Thomas Malthus predicted an eminent economic disaster based on a comparison between exponentially growing population and polynomial growth of resources. He erroneously predicted disaster would begin by 1825 and that population growth, if not altered, would lead to mass starvation by 1900 in a world which would only have enough food for 30% of the population. More recently, in 1970 Paul Ehrlich predicted, in his controversial book "The Population Bomb" [10], that a Malthusian-type disaster would occur by the year 2000. In retrospect it appears that these and numerous other similar predictions failed because they were unable to account for changes in technology and for the degree of nonlinearity of the systems involved.

In an ideal setting, results from dynamical systems models should be compared to results from experiments conducted in a controlled environment. This is certainly not the case when using dynamical systems to predict human population - resource dynamics. Moreover, when modelling human populations there is a legitimate question as to whether equations can even be reasonably determined by fundamental principles governing human behavior. Moreover, the rules governing the dynamics of a given population depend on social norms regarding reproduction, government controls on resources, and other factors which vary greatly between societies. Yet, tools from economics in conjunction with mathematics do have the ability to describe and predict collective human behavior at least in the short-term.

The closest one can get to a "controlled experiment" with human population dynamics is to examine civilizations that developed in isolation or with limited contact over an extended period of time. Modelling these human civilizations not only provides insight into the given civilization, but has the potential to be useful in understanding human population dynamics more generally.

There has been much recent activity in modelling human civilizations using differential and discrete equations. In [6], Brander and Taylor investigate the collapse of Easter Island using differential equations. J. Marty Anderies suggests a general framework for such differential equations models of human populations with a simple economy in [1], shown as Equation 1 below. Anderies employs dynamical systems models in [2] to model human populations and resources use. In a multi agent model, each population member is considered individually as a discrete unit. Robert Axtel uses these models to study the collapse of the Kayenta Anasazi civilization in [3]. Axtel and J. M. Epstein study multi agent models more generally in [4]. These models, which have been increasing in popularity especially in the economics literature, are similar in spirit to the well-known game of life. The difference between the multi agent models and the single entity models is akin to modelling a gas by modelling every individual molecule or using the ideal gas law. Other models take into account spatial distribution of resources. The excellent text [16] by Peter Turchin provides an overview of various population models, and Turchin's text [17] investigates applications to a variety of human populations. Many of these models fit into the framework of ecological economics, where the focus is on economics of a population and its interaction with the ecology.

Jared Diamond's very nice book "Collapse" [8] gives a good overview of the process of collapse in ancient civilizations, as best as can be understood from archeological evidence available. Diamond identifies several common causes for collapse; environmental overuse, decrease in friendly neighbors (trade disruption), increase in unfriendly neighbors (war), climate change (such as drought), and the civilization's response to the changing environment. It would be interesting to investigate each cause with mathematical models, looking for "signature properties" of each cause which would help identify the cause in a past civilization. For example, the figures in [5] suggest that a collapse caused by environmental destruction creates a population graph with a specific shape: a long slow exponential growth followed by a drastic turn and very fast period of collapse. A climate change may be more likely to create a time of stable population near equilibrium followed by a quick collapse. This would aid in determining the cause of collapse for various civilizations. Determining the cause of collapse for ancient civilizations is one of the most important questions in archeology, and one of the most hotly debated.

The differential equations and discrete dynamical systems commonly considered for ancient civilizations are derived from economics and biological population models. Each model typicaly has a discrete version and a continuous version. In many cases, particularly when growth rates are small, both versions are equally valid. If other cases there is a clear preference for either continuous or discrete model. For example, if one of the population's reproduction cycle occurs on an annual basis then a discrete model is preferred. For now, we provide some general framework from the point of the differential equations models. A basic form suggested for modelling one human population and one resource in [1] by Anderies is

$$\begin{aligned} \frac{\mathrm{d}P}{\mathrm{d}t} &= G(H,R)P \\ \frac{\mathrm{d}R}{\mathrm{d}t} &= \rho(R) - H(R,P). \end{aligned} \tag{1}$$

Here, $G(H,R)$ is the growth rate of the population (equivalently, G is the difference between the per person birth and death rates), $\rho(R)$ is the growth rate of the resources and $H = H(R,P)$ is the rate at which resources are harvested. Such models of course focus on the interaction between the population and environment in a stable climate, without regard for trade, war, or disease.

As and example where this general framework is used, Brander and Taylor [6] studies the model given by equation 2 for the study of the population of Easter Island. They choose the logistic form $\rho(R) = cR(1 - R/K)$, their harvesting rate is proportional to PR, and for G, they use the linear function $G(H, R) = (b - d + \phi R)$ where b is the birth rate, d is the death rate, and ϕ is a constant. (The function $P(t)$, in Anderies' work and in the work of some other researchers in this field, is the labor pool, whereas we consider, instead, the entire population.)

$$\begin{aligned} \frac{\mathrm{d}P}{\mathrm{d}t} &= (b - d + \phi R)P \\ \frac{\mathrm{d}R}{\mathrm{d}t} &= cR(1 - R/K) - hPR. \end{aligned} \tag{2}$$

This model is well-motivated from neoclassical economics in [6]. The authors also present a thorough analysis of parameter values for Easter Island and discuss a number of important economic issues involved in the collapse. However, in this model the origin is always either a saddle or a source with its stable and unstable sets on the axis. Thus, there are no solutions the begin in the first quadrant and have $R \to 0$. While this model can exhibit a growth and decline of the population as part of a large periodic cycle, it does not have the proper long-term behavior for a collapse. This is part of the motivation for models (3) and (4) which we investigate in this article.

2. The Model

In [5], the authors present a differential equation, shown below as Equation (3), modeling an isolated population and its resource such as in the human population on Easter Island. A complete classification of the qualitative behavior for this continuous model is demonstrated in [5]. In addition, biologically motivated parameter values are provided and numerical solutions using these values closely match archeological evidence for Easter Island. The combination of proper economics derivation and fitting the observed behavior indicated that Equation 3 is a good model for the Easter Island population. In these equations, the parameters a, c, K, and h represent the intrinsic growth rate of the population, the intrinsic growth rate of the resource, the resource carrying capacity, and the harvesting rate respectively. The units of the population are in number of animals and the units of the resource are such that one unit of resources is sufficient to sustain one unit of population for one year. Observe that in Equation (3), the the population is modeled by a logistic equation with the resource determining the carrying capacity, and the resource is modelled by a logistic equation with harvesting.

$$\begin{aligned} \frac{\mathrm{d}P}{\mathrm{d}t} &= aP\left(1 - \frac{P}{R}\right) \\ \frac{\mathrm{d}R}{\mathrm{d}t} &= cR\left(1 - \frac{R}{K}\right) - hP. \end{aligned} \tag{3}$$

The motivation for these equations is as follows. We assume that the resource, say trees, animals, or crops, is governed by a logistic equation in the absence of people. We assume that the per capita consumption of the resource by people does not depend on the amount of the resource. This results in the harvesting rate of hP in Equation (3). This differs from the harvesting rate hPR which is often used in modeling animal populations. (See [16].) Our harvesting rate is more appropriate in cases where the population has easy access to the resources. This is appropriate for the case of humans on Easter Island whose governing resource is trees, or the case of the Maya in Mesoamerica where the population was extremely dense. Our harvesting rate is also reasonable for modeling animal populations when the prey are abundant. We also assume that the population is governed by a logistic equation with the resources comprising the carrying capacity. A detailed justification for these equations, including a comparison to neoclassical economic models, is presented in [5] and we shall not repeat it here.

It is our purpose in this paper to study the discrete version of this equation, given in Equation (4) where we assume $K = 1$. We employ the standard technique of discritizing the continuous model by using the formulas for the rates of change as the formulas for the amount of change in a single year. Some of the resources consumed by the population of Easter Island, such as migratory birds and fish, reproduce on an annual cycle, suggesting that a discrete model should be as valid as a differential equations model. In addition, the discrete equation 4 match archeological data very well as shown in Figure 1. In this model it is possible for the population and resource to both go to zero as time goes to infinity as in a collapse. It is also possible in the model for the population and resource to leave the first quadrant, which also corresponds to a collapse. A model similar in form to Equation 4 was used in [9] to study the populations of wolves and moose in Canada. The reproductive cycles of these populations also governed on an annual cycle. The paper [9] offered extensive analysis of relevant parameter values and some numerical evidence of the validity of this model, but did not present analysis of the equations. In addition to being useful, Equation (4) exhibits rich behavior of attractors, fractal Julia sets, and chaos.

The discretization of Equation (3) is

$$(4) \qquad \begin{aligned} P_{n+1} &= P_n + aP_n\left(1 - \frac{P_n}{R_n}\right) \\ R_{n+1} &= R_n + cR_n\left(1 - \frac{R_n}{K}\right) - hP_n, \end{aligned}$$

where $a, c, h > 0$.

The discrete population Model (4) was developed to investigate the population dynamics of Easter Island. The model does achieve its original goal as can be seen in Figure 1, depicting the population predicted from the model together with data points estimated from archeology. (The archeology gives us not only a few data points, but also, more significantly, a the length of time of the extended growth period and the collapse.) The parameters are $a = 0.044$, $c = 0.001$, $h = 0.018$, $K = 70,000$, and the initial conditions are $P_0 = 50$, $R_0 = 70000$. The value for K is easy to estimate from the size and fertility of Easter Island. The value for a is in the standard range for pre-industrial revolution civilizations. (See [7].) The values for c and h are more difficult to estimate, but are reasonable for tree growth and harvesting rates.

It is important to observe that not only does our model match the archeological data and qualitative description, it does so with realistic parameter values. For example, the 1-dimensional logistic model can experience a growth and collapse, but not with parameter values close to human growth rates. Moreover, the one dimensional logistic equation could not experience a growth on collapse matching the qualitative timescale provided by archeology for any parameter values.

For simplicity of notation we assume that $K = 1$, which is equivalent to taking the units of P as percentage of total sustainable population. We often write

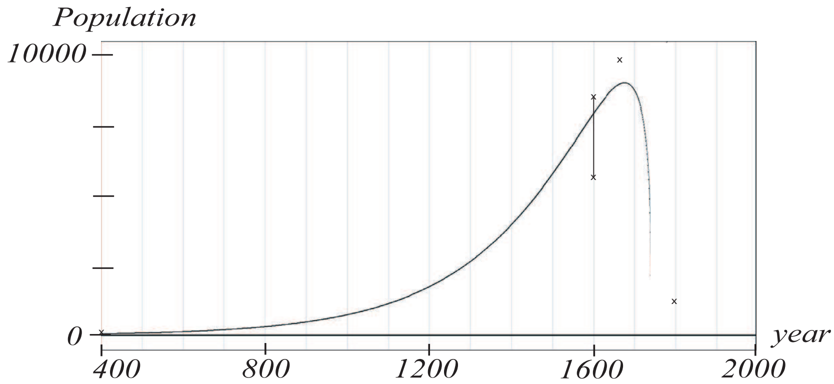

FIGURE 1. The graph of population verses time using Model (4) applied to Easter Island. Each 'x' is a data point or data range approximated through archeological evidence.

System (4) as

$$\begin{pmatrix} P_{n+1} \\ R_{n+1} \end{pmatrix} = F \begin{pmatrix} P_n \\ R_n \end{pmatrix}, \qquad F \begin{pmatrix} P \\ R \end{pmatrix} = \begin{pmatrix} P + aP\left(1 - \dfrac{P}{R}\right) \\ R + cR\,(1 - R) - hP \end{pmatrix}.$$

Let $F_P(P, R)$ denote the first coordinate of $F(P, R)$ and let $F_R(P, R)$ denote the second coordinate. For an initial condition (P_0, R_0), denote the n^{th} iterate by $(P_n, R_n) = F^n(P_0, R_0)$.

3. Local Analysis

The two equilibria of System (4) are $(P, R) = (0, 1)$ and $(P_e, R_e) = \left(1 - \frac{h}{c}, 1 - \frac{h}{c}\right)$. These two equilibria and the singularity at $(P, R) = (0, 0)$ will each be analyzed for linear stability in turn.

First let us show that any neighborhood of the singularity $(P, R) = (0, 0)$ is unstable for all positive parameters, a, c, and h by considering the $P = 0$ axis. One can see that the origin is not stable by noting that for any small R, $F_R(0, R) > R$. Thus, in the absence of a human population, the resource does not become extinct on its own except in the case of very large growth rates. In the absence of a human population the resource dynamic behaves as the logistic map.

The second equilibrium of System (4), $(P, R) = (0, 1)$, will also be shown to be linearly unstable. In order to demonstrate that instability, the Jacobian $\mathbf{J}$ will be needed.

$$\mathbf{J} = \begin{bmatrix} a - 2a\frac{P}{R} + 1 & a\frac{P^2}{R^2} \\ -h & c - 2cR + 1 \end{bmatrix}$$

The Jacobian will be evaluated at the equilibrium in question, $(P, R) = (0, 1)$. Linear stability will equate to both eigenvalues of the Jacobian having magnitude less than 1.

At the equilibrium $(P, R) = (0, 1)$, the Jacobian is

$$\mathbf{J} = \begin{bmatrix} a + 1 & 0 \\ -h & 1 - c \end{bmatrix}.$$

The $a + 1$ eigenvalue of this lower triangular matrix is greater than 1 for any choice of $a > 0$ and thus this equilibrium is linearly unstable. The modelling interpretation is of course that when the settlers first arrive on the island their little colony has a chance to grow. Their arrival on the island can be seen as a perturbation from the equilibrium point $(P, R) = (0, 1)$.

Now we consider the stability of the equilibrium $(P_e, R_e) = \left(1 - \frac{h}{c}, 1 - \frac{h}{c}\right)$. In order for this equilibrium to exist in the first quadrant we require $h < c$. The Jacobian $\mathbf{J}$ evaluated at the equilibrium of (P_e, R_e) is

$$\mathbf{J} = \begin{bmatrix} 1 - a & a \\ -h & -c + 2h + 1 \end{bmatrix}.$$

In order to facilitate the local stability analysis we will use the trace-determinant plane in lieu of the direct calculation of the eigenvalues in terms of the three parameters. (See [15].)

The trace of the Jacobian is $tr(\mathbf{J})$ and the determinant of the Jacobian is $\det(\mathbf{J})$. The stability triangle in the trace-determinant plane is bounded by the inequalities

$$\begin{aligned} \det \mathbf{J} &< 1 \\ tr(\mathbf{J}) - 1 &< \det(\mathbf{J}) \\ -tr(\mathbf{J}) - 1 &< \det(\mathbf{J}). \end{aligned}$$

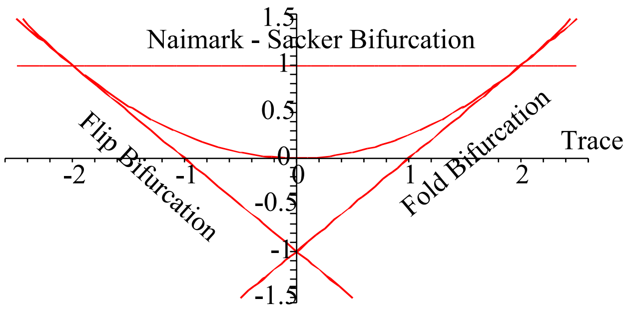

FIGURE 2. The stability triangle.

The stability triangle will now be used to analyze the stability of the equilibrium $(P_e, R_e) = \left(1 - \frac{h}{c}, 1 - \frac{h}{c}\right)$. The $tr(\mathbf{J}) = 2 - a - c + 2h$ and the $\det(\mathbf{J}) = h(2 - a) + (1 - a)(1 - c)$ are generated from the Jacobian evaluated at that equilibrium. The upper side of the stability triangle, which corresponds to a Neimark-Sacker bifurcation, is given by the inequality

$$h(2 - a) + (1 - a)(1 - c) < 1. \tag{5}$$

The right side of the stability triangle, which corresponds to a fold bifurcation (also called a period doubling bifurcation), is given by

$$2 - a - c + 2h - 1 < h(2 - a) + (1 - a)(1 - c).$$

The left side of the stability triangle, which corresponds to a flip bifurcation, is given by

$$-(2 - a - c + 2h) - 1 < h(2 - a) + (1 - a)(1 - c).$$

These three equations simplify to

$$\begin{aligned} h(2 - a) + (1 - a)(1 - c) &< 1, && \text{N.-S. Bifurcation} \\ h &< c, && \text{Fold Bifurcation} \\ (2 - a)(c - h - 2) &< 2h, && \text{Flip Bifurcation.} \end{aligned}$$

If the above three inequalities are satisfied the equilibrium is linearly stable. To further refine the three stability conditions above consider the right side boundary of the stability triangle. The condition $c > h$ must already be met in order for the equilibrium $(P_e, R_e) = \left(1 - \frac{h}{c}, 1 - \frac{h}{c}\right)$ to be in the first quadrant and it is hence realistic given our model.

Because the population in a given region has the most control over the harvesting parameter h, the two remaining inequalities will be combined to produce a stability condition on h. The resulting stability zone, assuming $a < 1$, is

$$\frac{(a-2)(c-2)}{a-4} < h < \frac{1-(1-a)(1-c)}{2-a}. \tag{6}$$

Of the three parameters, a is known with the most confidence. Anthropological studies estimate $a \simeq 0.0045$. (See [5].) Observe that for this a value Equation 6 rounded to 2 significant figures becomes

$$0 < c - 2h < 2.$$

The stability zone in the $c - h$ plane is seen in Figure (3). For $a = 0.0045$ the intersection between the lines $h = \frac{(a-2)(c-2)}{a-4}$ and $h = \frac{1-(1-a)(1-c)}{2-a}$ occurs at the biologically irrelevant value of $c \approx 1773$.

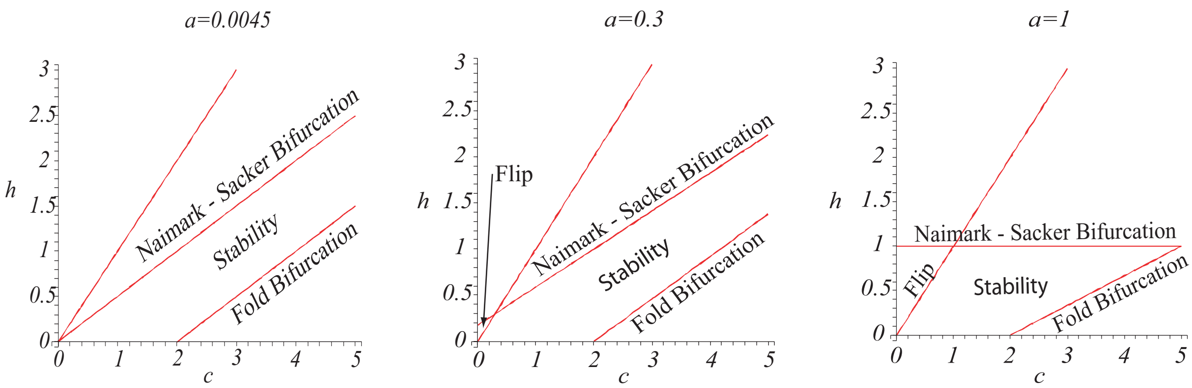

FIGURE 3. The stability region for $a = 0.0045$, $a = 0.3$, and $a = 1$.

Notice that any stable equilibrium becomes unstable when h increases. This matches our intuition about the model in that if the island's population harvests too much of the resource, the equilibrium will be unstable. Surprisingly enough the same can be done by increasing the resource growth rate c. The island's population can increase the resource growth rate through superior farming techniques such as irrigation, and this technological advance will result in the destabilization of the equilibrium point. This destabilization is a fold bifurcation.

The intersection of the $h = c$ boundary and the $h = \frac{1-(1-a)(1-c)}{2-a}$ upper boundary occurs at the point where $h = a = c$. For resource growth rates c less than the population growth rate a, increasing the harvesting rate pushes the equilibrium point to the origin and both resource and population go extinct simultaneously. For resource growth rates c greater than the population growth rate a, increasing the harvesting rate pushes the equilibrium point to a Neimark-Sacker bifurcation.

Solving for the intersection of the two boundary conditions shows that for resource growth rates than are too large ($c > \frac{a^2-4a+8}{a}$) the equilibrium will be unstable for any harvest rate.

4. The Neimark-Sacker bifurcation

Let's turn our attention to the Neimark-Sacker bifurcation of the stability triangle. As in Equation (5), this corresponds to the boundary with

$$h(2-a)+(1-a)(1-c)=1.$$

We focus on the value of h because, as before, we assume that the population has the most control over the harvesting rate. If we fix the values of a and c and slowly change the value of h then we can see that we will leave the stability triangle on this boundary when

$$h=\frac{a+c-ac}{2-a}. \tag{7}$$

We also need that $-2 < tr(\mathbf{J}) < 2$ at this h value, (see Figure 3.)

$$-2 < 2-a-c+2h < 2. \tag{8}$$

Substituting (7) into (8) yields the inequalities

$$\frac{a+c}{2}-2 < \frac{a+c-ac}{2-a} < \frac{a+c}{2}.$$

After simplification, we obtain

$$a < c < a-4+\frac{8}{a}. \tag{9}$$

We illustrate this inequality for $0.5 < a < 2$ in Figure 5.

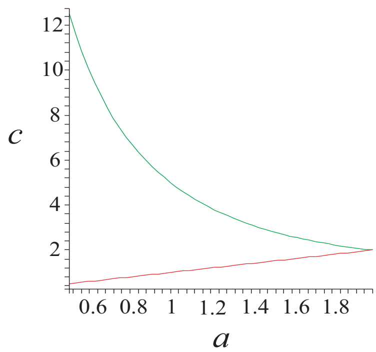

Figure 4. The graphs of $c=a$ and $c=a-4+\frac{8}{a}$.

Our estimation was $a \simeq 0.0045$. This leaves a fairly wide window for c, as we can see from Inequality 9, and in turn, this means that the Neimark-Sacker bifurcation will exist for a large part of the parameter domain.

We can see that as long as inequality (9) stands, at $h=(a+c-ac)/(2-a)$ the fixed point at $(1-h/c, 1-h/c)$ loses its stability and becomes an unstable fixed point. The Neimark-Sacker bifurcation theorem establishes the existence of a closed invariant curve around the (now unstable) fixed point. This bifurcation is illustrated in Figure 6 for the parameter values $a=0.0045$, $c=3$ with $h=1.495$, $h=1.498$, and $h=1.499$.

A very interesting question at this point is the disappearance of the closed invariant curve as we slowly increase the value of h. Lately, there has been considerable interest in this phenomenon, especially from the computational point of view. (See [11].) As we increase the value of h, the invariant closed curve gradually develops cusps. Later a periodic orbit contained on this invariant curve also undergoes

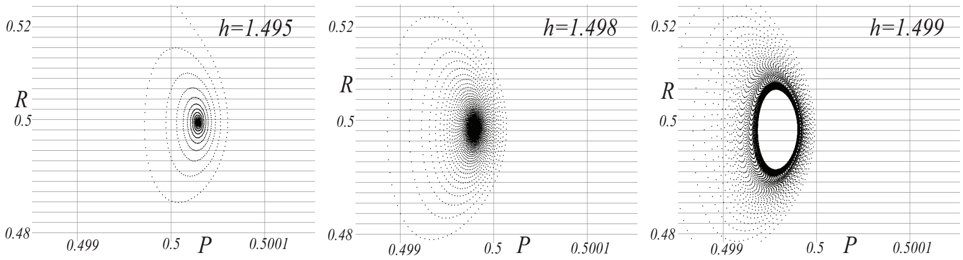

FIGURE 5. Three phase planes are shown with $a = 0.0045$, $c = 3$ and h-values near the Neimark-Sacker bifurcation.

a secondary Neimark-Sacker bifurcation, then beyond a certain parameter value numerical studies indicate chaotic behavior. (See Figure 12.) The dynamics of this procedure is not known in its entirety, but it is known that in the noninvertible case (such as ours) the invariant curve might intersect the locus on which the Jacobian of the linearized map becomes singular. The angle of intersection between a saddle unstable manifold and this critical curve underpins the transition of the local image of the invariant curve.

5. Numerical Bifurcation Analysis

There are three parameters, a, c, and h that determine the behavior of the system. We break our analysis into 3 cases depending on the value of a. Figures 6 through 12 show bifurcation diagrams and accompanying phase planes for the population growth rates $a = 0.0045$ (pre-industrial revolution humans), $a = 0.3$ (medium sized animals), and $a = 1$ (small animals).

Corresponding to each value for a, we provide a plot of the stability region in the (c, h)-parameter plane. Accompanying each plot of the parameter plane are multiple bifurcation diagrams. The parameter values for each bifurcation diagram are indicated in the parameter plane by a vertical line. Each bifurcation diagram shows P on the vertical axis and h on the horizontal axis. The bifurcation diagram was generated by sampling 2500 values for h between 0 and 1.6. For each value of h, using the indicated values of a and c, 10,000 iterates of F were calculated and the iterates P_{9000} through P_{10000} were plotted above the given h value.

In selected bifurcation diagrams, vertical arrows are shown indicating h-values of particular interest. For each of these h-values, a plot of the attractor in the P, R-plane is also shown in a figure.

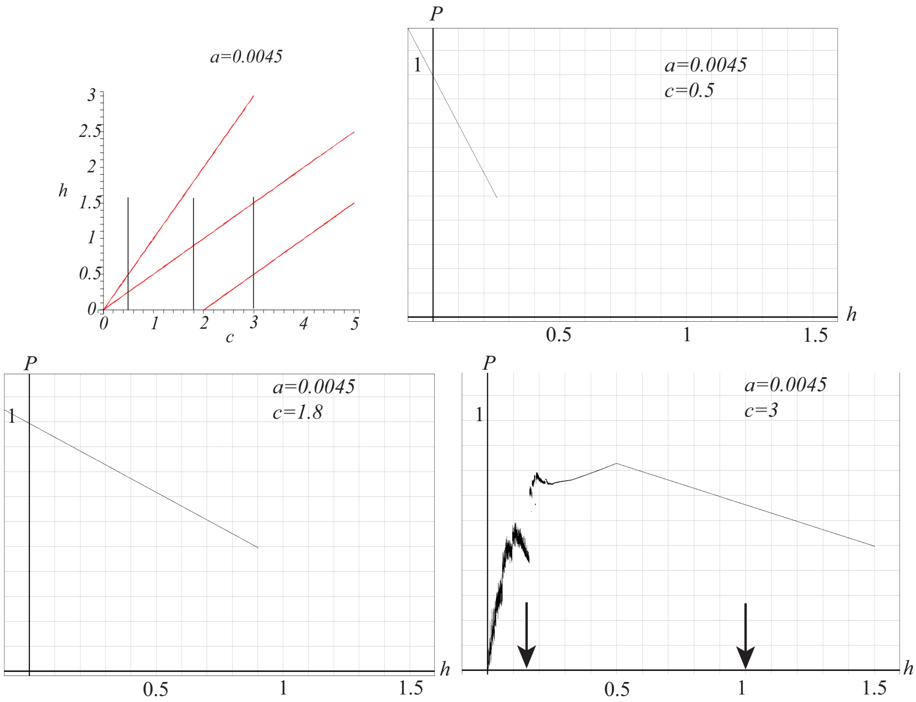

FIGURE 6. The first plot is the stability region in the c, h-parameter plane for $a = 0.0045$ with lines indicating the parameter values for the bifurcation diagrams. Bifurcation diagrams are shown for $a = 0.0045$ with $c = 0.5$, $c = 1.8$, and $c = 3$. The arrows in the diagram for $c = 3$ indicate the parameter values for the attractors that are shown in Figure 7.

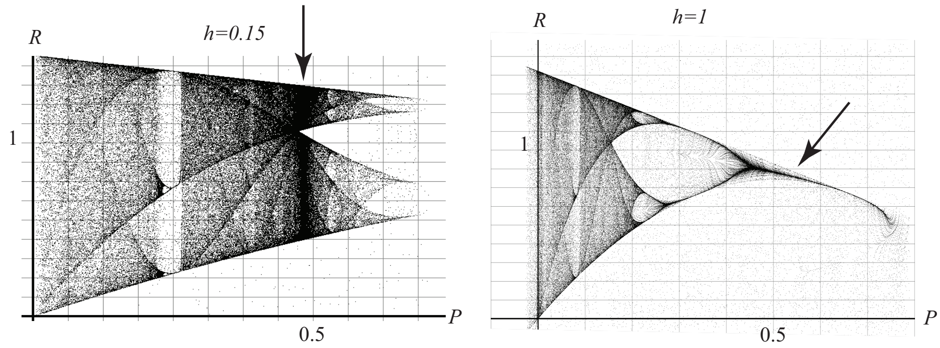

FIGURE 7. The first 1000 iterates of 5000 initial conditions for $a = 0.0045$, $c = 3$ and $h = 0.15$ and $h = 1$. These parameter values are indicated by the arrows in the bifurcation diagram in Figure 6. In the case with $h = 0.15$ the attractor is a chaotic region indicated by the arrow. In the case with $h = 1$ the attractor is an equilibrium point, also indicated by an arrow. In each case, the set resembling a bifurcation diagram for the logistic equation forms a "stable set" for the attractor.

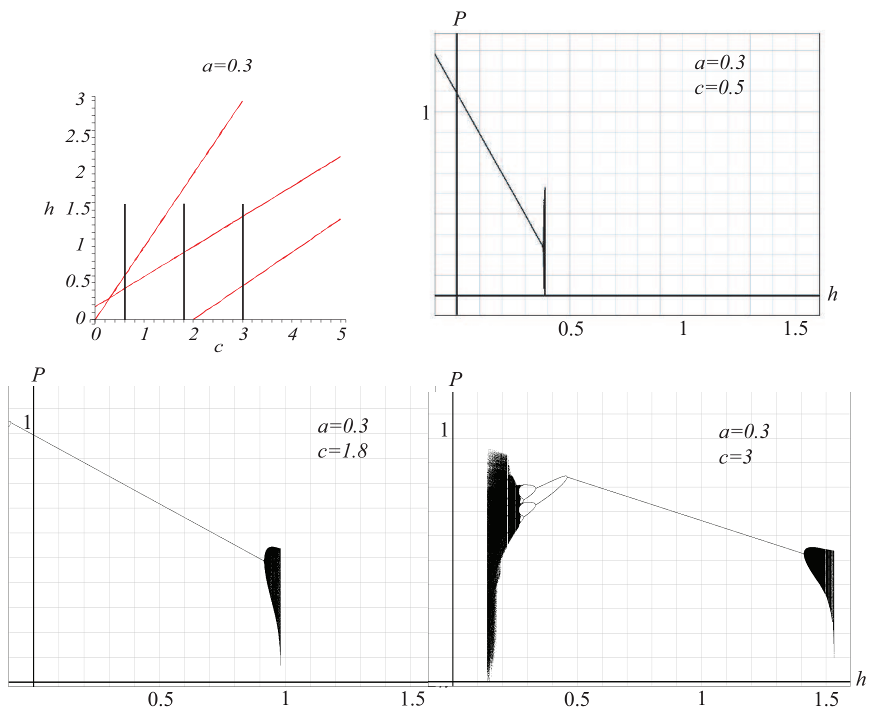

FIGURE 8. The first plot is the stability region in the c, h-parameter plane for $a = 0.3$ with lines indicating the parameter values for the bifurcation diagrams. Bifurcation diagrams are shown for $a = 0.3$ with $c = 0.5$, $c = 1.8$, and $c = 3$. Observe the nontrivial attractors that occur just outside the stability region.

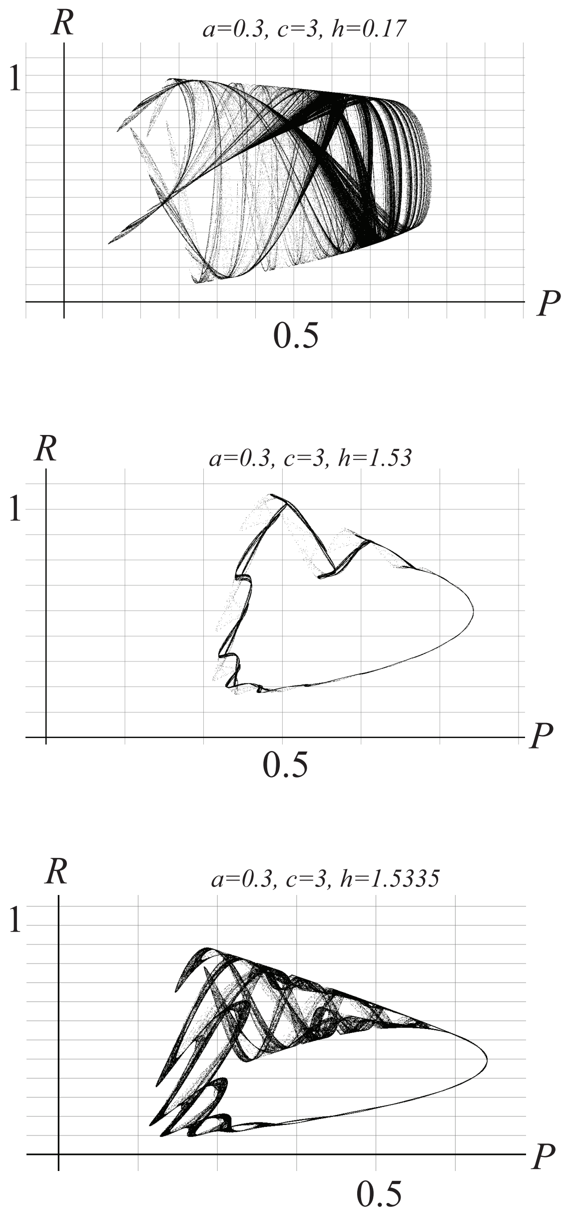

Figure 9. The attractor for the system with $a = 0.3$, $c = 3$, and with h equal to 0.17, 1.53, and 1.5335. Note the indications of homoclinic intersections and horseshoes.

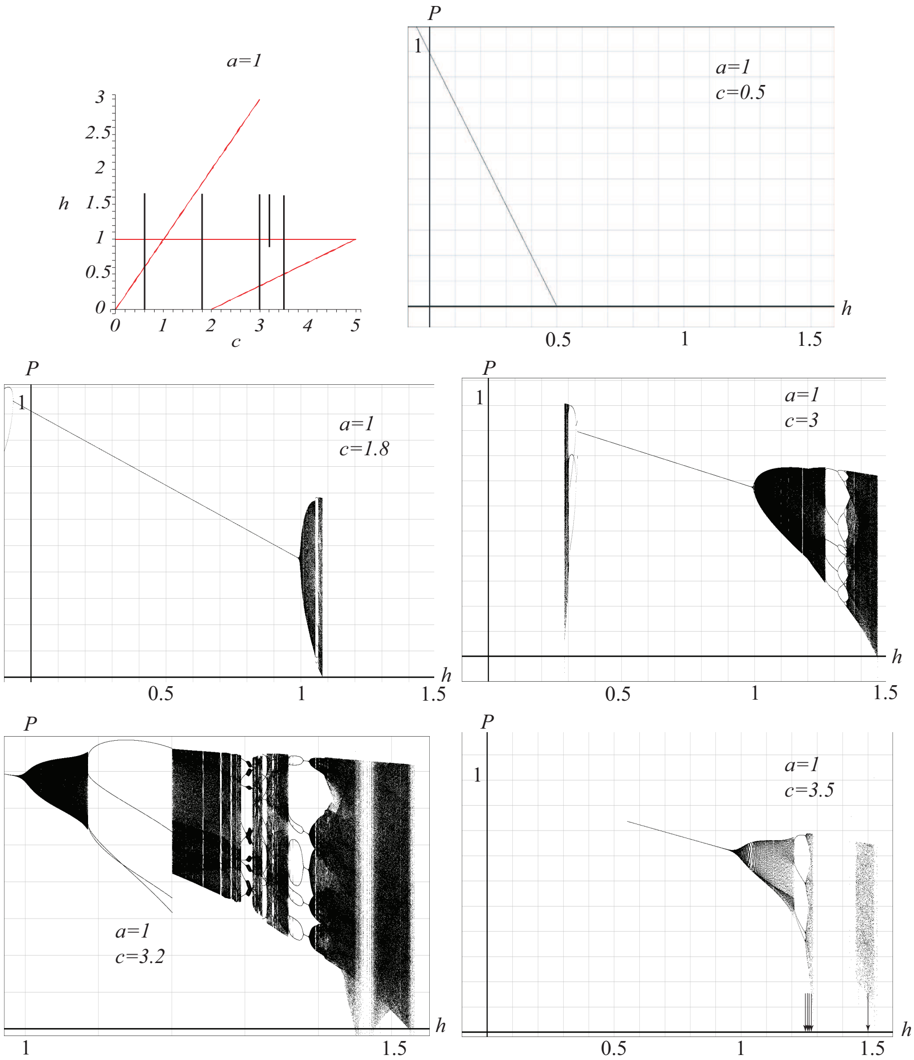

FIGURE 10. The first plot is the stability region in the c, h-parameter plane for $a = 1$ with lines indicating the parameter values for the bifurcation diagrams. Bifurcation diagrams are shown for $a = 1$ with $c = 0.5$, $c = 1.8$, and $c = 3$, as well as $c = 3.2$ and $c = 3.5$. The arrows in the diagram for $c = 3.5$ indicate the parameter values for the attractors shown in Figures 11 and 12.

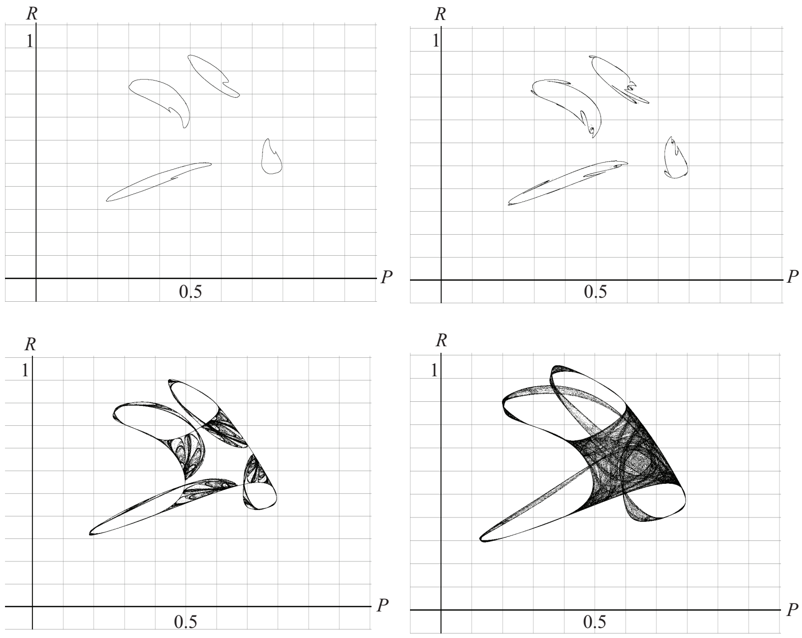

FIGURE 11. The attractor for the system with $a = 1$, $c = 3.5$, and with h ranging from 1.27 to 1.278.

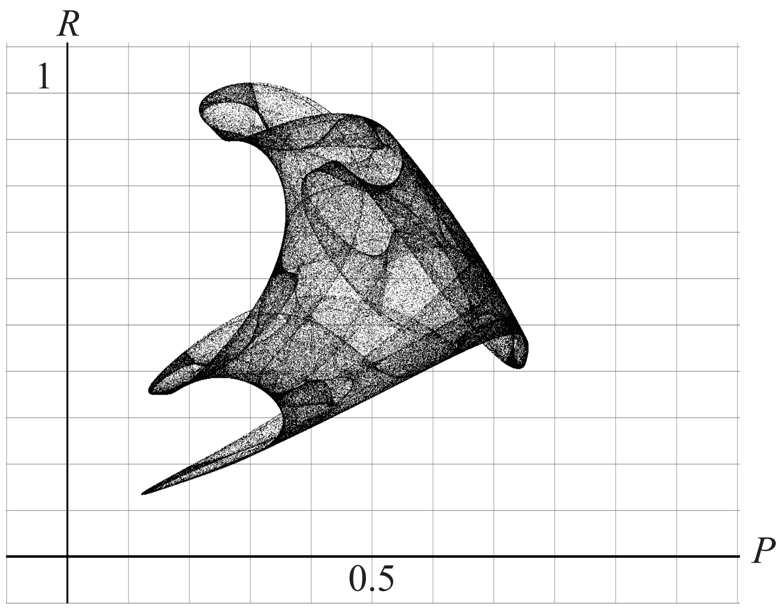

FIGURE 12. The attractor for the system with $a = 1$, $c = 3.5$, and $h = 1.5$.

6. Global Analysis and Basins of Attraction

In this section we study the global behavior of the system. We focus on the basin of attraction of the attractor, which constitutes the set of initial conditions that do not lead to extinction. (The attractor may be a stable equilibrium point or it may be a more complicated set. The basin of attraction is often also called the Julia set.) The basin of attraction is not the entire first quadrant. As is common for discrete systems, the basin of attraction is fractal in nature, and hence is difficult to determine precisely. In this section we provide some qualitative analysis of its size and shape for various parameter values.

Let $Z_P = \{(P,R) \,|\, F_P(P,R) = 0\}$ denote the zero set of F_P and $Z_R = \{(P,R) \,|\, F_R(P,R) = 0\}$ denote the zero set of F_R. Observe that Z_P is is the pair of lines

$$Z_P = \{P = 0\} \cup \{P = R(1 + 1/a)\}$$

and Z_R is the parabola

$$Z_R = \{P = \frac{c}{h} R(1 + 1/c - R)\}.$$

So F maps Z_R to the $P-$axis and Z_P to the $R-$axis.

Also useful are the sets

$$E_P = \{(P,R) : F_P(P,R) = P\} = \{P = 0\} \cup \{P = R\}$$

and

$$E_R = \{(P,R) : F_R(P,R) = R\} = \{P = \frac{c}{h} R(1 - R)\}.$$

Of course the points of intersection of E_P with E_R are the equilibrium points. These sets are shown in Figure 14.

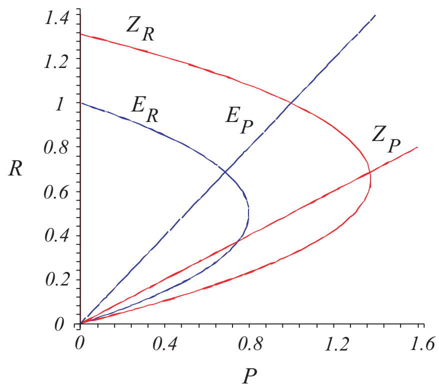

Figure 13. The sets Z_P, Z_R, E_P and E_R for $a = 1$, $c = 3.2$, and $h = 1$.

The complement of $Z_P \cup Z_R$ in the first quadrant has either 3 or 4 components.

PROPOSITION 1. *The complement of $Z_P \cup Z_R$ in the first quadrant has 4 components if*

$$\left(\frac{a+1}{a}\right) h - c - 1 < 0.$$

Otherwise, the complement of $Z_P \cup Z_R$ in the first quadrant has 3 components.

Moreover, using the labelling scheme from Figure 15,

- *F maps A to the first quadrant.*
- *F maps B to the second quadrant.*

- *F maps C to the third quadrant.*
- *F maps D to the fourth quadrant.*

Proof. This is a straightforward calculation observing that the line $P = R(1+1/a)$ intersects the parabola $\{P = \frac{c}{h}R(1+1/c-R)\} = Z_R$ in exactly one point with $P, R > 0$ if $\left(\frac{a+1}{a}\right)h - c - 1 < 0$ and otherwise they do not intersect at any points with $P, R > 0$. The claim regarding the regions A, B, C, and D follows easily from checking the inequalities $F_P(0,0) < 0, F_P(0,0) > 0, F_R(P,R) < 0$, and $F_R(P,R) > 0$. □

Observe that the map F extends continuously to the origin from within A by defining

$$F(0,0) = (0,0).$$

From now on we assume that $F(0,0) = (0,0)$ so that F is continuous on $\overline{A}$, the closure of A. Observe also that F is now continuous on the $R-$axis.

COROLLARY 1. *Let (P,R) be any point in $\mathbb{R}^2$. Then $F(P,R)$ is in the first quadrant if and only if $(P,R) \in A$.*

Proof. For (P,R) in the first quadrant, this follows from Proposition 1. If (P,R) is not in the first quadrant then either $P < 0$, $P \leq R$ or $R < 0$, $R \leq P$. If $P < 0$, $P \leq R$ then $F_P(P,R) < 0$ and if $R < 0$, $R \leq P$ then $F_R(P,R) < 0$. □

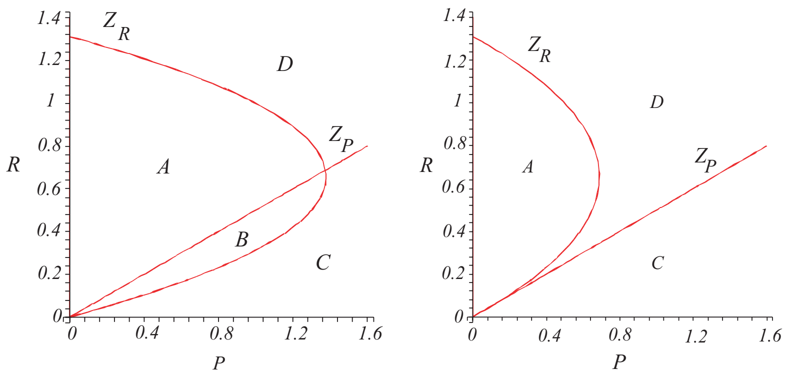

FIGURE 14. The regions A, B, C, and D. In the first plot, the parameters are $a = 1$, $c = 3.2$, and $h = 1$. In the second plot the parameters are $a = 1$, $c = 3.2$, and $h = 2$.

7. The Julia Set

The goal of this section is to determine the topology of the Julia set for F. The Julia set is defined to be the set of initial conditions whose positive orbits remain in the first quadrant and are bounded. It serves as the basin of attraction for all attractors in the first quadrant. Figure 15 shows the Julia set together with the sets Z_P, Z_R, E_P, and E_R for $a = 1$, $c = 3.2$, and $h = 0.9$.

Our first result regarding the Julia set follows directly from Corollary 1.

PROPOSITION 2. *The Julia set is contained in the region A.*

PROPOSITION 3. *The map F restricted to the $R-$axis is conjugate to a logistic map $l(x) = (1+c)x(1-x)$.*

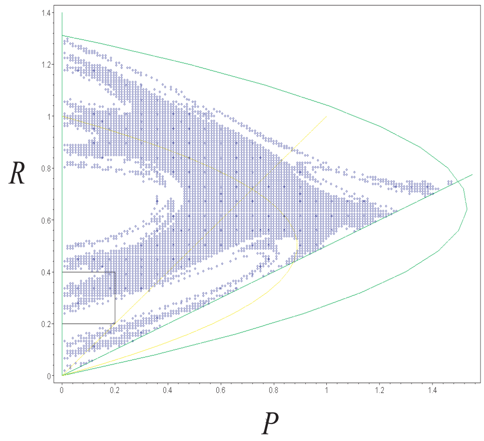

FIGURE 15. The Julia set for $a = 1$, $c = 3.2$, and $h = 0.9$.

Proof. Observe, first, that the $R-$axis is invariant under F,

$$F(0, R) = (0, R + cR(1 - R)).$$

Define $h : \mathbb{R} \to \mathbb{R}$ by

$$h(R) = \frac{c}{1+c}R.$$

To show that $h(F(0, R)) = l(h(R))$,

$$\begin{aligned} h(F(0, R) &= \frac{c}{1+c}[R + cR(1 - R)] \\ &= \frac{c}{1+c}[(1 + c)R(1 - \frac{c}{1+c}R)] \\ &= (1 + c)\frac{c}{1+c}R(1 - \frac{c}{1+c}R) \\ &= (1 + c)h(R)(1 - h(R)) \\ &= l(h(R)). \end{aligned}$$

□

COROLLARY 2. *The Julia set intersected with the $R-$axis is*

- *the interval* $[0, 1 + 1/c]$ *if* $c \leq 3$, *or*
- *a Cantor set contained in the interval* $[0, 1 + 1/c]$ *if* $c > 3$.

Proof. The Julia set for the logistic map $l(x) = (1+c)x(1-x)$ is a is a Cantor set if $c > 3$ and is an interval $[0, 1]$ if $c \leq 3$. The corollary follows then from Proposition 3 since h takes $[0, 1 + 1/c]$ to $[0, 1]$. □

PROPOSITION 4. *Let* $I = [0, 1 + 1/c]$ *and let* $x_n = (P_n, R_n), n > 0$ *denote an orbit for* F. *If* $d(x_n, C) \to 0$ *as* $n \to \infty$ *then* $x_n \to (0, 0)$ *as* $n \to \infty$. *Hence,* $(0, 1 + 1/c]$ *does not contain a stable set.*

Proof. This follows from the observation that $F_P(P, R) > P$ if $P > R$. □

Suppose that $\left(\frac{a+1}{a}\right) h - c - 1 < 0$ and $c > 3$. The Julia set for a set of parameters in this range is shown in Figure 15. Observe that the origin has three preimages, $O_1 = (0, 0)$, $O_2(0, 1+1/c)$, and $O_3 = ((1+1/a)(h+h/a-c-1)/c, (h+h/a-c-1)/c)$. Let α be the arc in Z_P from O_1 to O_2, β be the arc in Z_R from O_2 to O_3, and γ be the arc in Z_P from O_3 to O_1.

Since $c > 3$, the midpoint of α is mapped to a point outside of A. Hence a neighborhood of the midpoint of α is mapped outside of A in one iteration. Let X be the maximal such neighborhood. Also, observe that β is mapped outside of A by F, so a neighborhood of β in A is mapped outside of A by F. Let Y be the maximal such neighborhood. (It is possible that $X = Y$, but this numerically does not appear to be the case for $a = 1, c = 3.2, h = 0.9$. See Figure 17.)

It is not difficult to determine the preimages of X and Y. Since X is mapped above Y (since $c > 3$), a neighborhood of Y contains points that get mapped to X by F. Because the map is two to one along the $R-$axis, the region X has two preimages; one above X and one below X. This is shown in upper left of Figure 17. One can estimate the preimages of these regions, and so on, as shown in the rest of Figure 17.

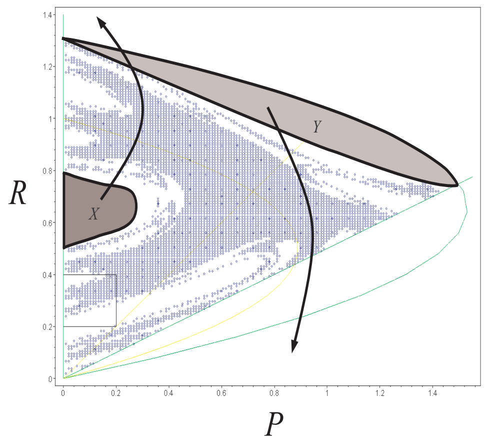

FIGURE 16. The Julia set for $a = 1$, $c = 3.2$, and $h = 0.9$.

8. Conclusion and Future Studies

Models of our type are useful in various applications. This is examined in general from a biology perspective in [16], and in a case similar to ours in [9]. For booming and crashing populations, a differential equations model similar to ours is studied in [5]. The papers [1] and [2] examine related models from an economics perspective. An advantage of our model is that it does not a priori force solutions to an equilibrium or periodic orbit. This makes extinction possible in our model.

Although comparison between numerical approximation and archeological data for Easter Island suggests the utility of our model, we have not investigated ecosystems in depth. Our analysis should, in the future, be followed up by a comparison of numerical approximations to data from various ecosystems, together with parameter fitting as in the biology literature. There is a variety of civilizations, such as the Maya in Mesoamerica and the Vikings in Greenland, to which our model could be applied. It is also likely that our model would be useful in studying animal populations involving extinction.

It would also be interesting, both in theory and in applications, to consider variations of our model. For example, it is of paramount interest to consider the case where the parameters are not constant, being either periodic functions of time or stochastic variables. This would have applications in economics, biology, archeology, and ecology.

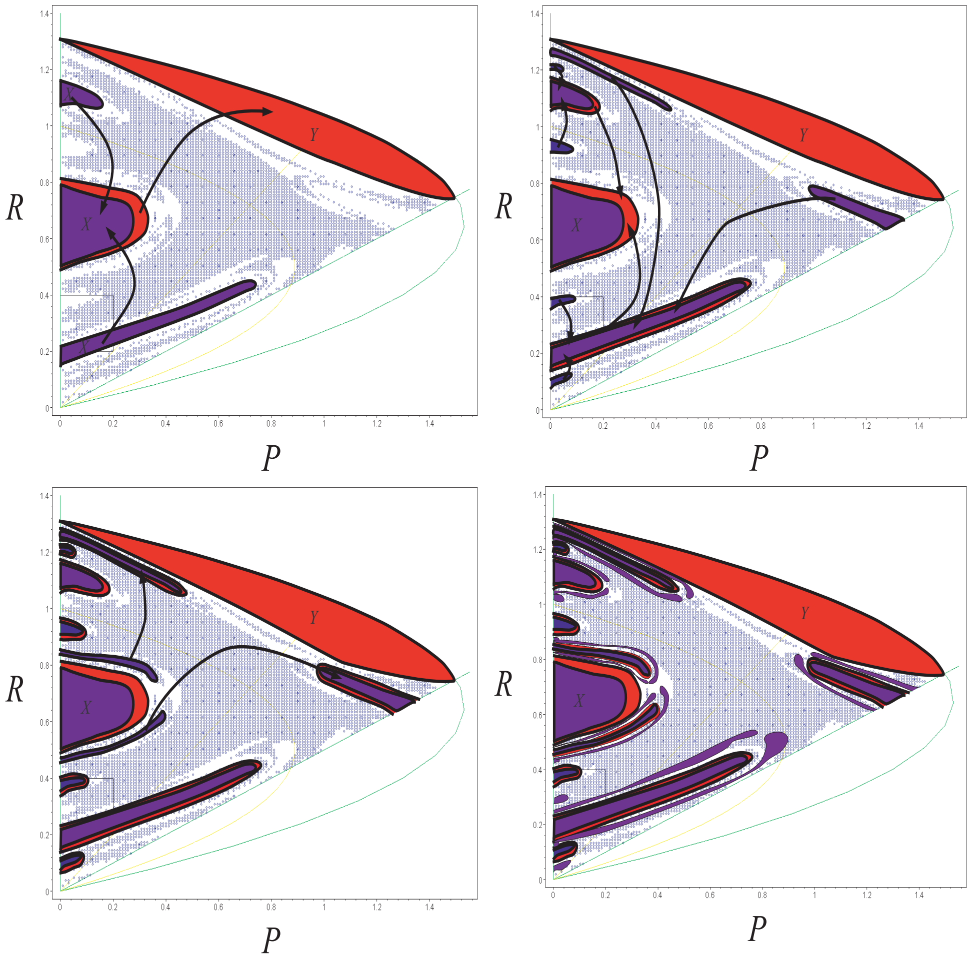

FIGURE 17. The Julia set for $a = 1$, $c = 3.2$, and $h = 0.9$ showing the escape sets.

REFERENCES

[1] J. M. Anderies, *On modeling human behavior and institutions in simple ecological economic systems*, Ecological Econimics, 35 (2000) pp. 393-412.

[2] J. M. Anderies, *Econimic development, demographics, and renewable resources: a dynamical systems approach*, Environment and Development Economics, 8 (2003) pp. 219-246.

[3] R. Axtell, *Population Growth and Collapse in a Multi-Agent Model of the Kayenta Anasazi in Long House Valley*, Proceedings of the National Academy of Sciences (2002)

[4] R. Axtell and J. M. Epstein, *Agent-Based Modeling: Understanding Our Creations*, The Bulletin of The Santa Fe Institute (Winter 1994)

[5] W. Basener and D. Ross, *Booming and crashing populations and Easter Island*, SIAM J. Appl. Math. 65 (2004/05), no. 2, pp. 684-701

[6] J. A. Brander and M. S. Taylor, *The simple economics of Easster Island: A Ricardo-Malthus model of renewable resource use*, American Economic Review, 88 (1998) pp. 119-138

[7] J. Cohen, How Many People Can the Earth Support. W. W. Norton and Company, 1995

[8] J. Diamond, Collapse, How Societies Choose to Fail or Succeed. Viking, 2005

[9] L.L.Eberhardt, *Applying difference equations to wolf predation*, Canadian Journal of Zoology, 76 (1998) pp.380-386.

[10] R. Ehrlich, *The Population Bomb*, Buccaneer Books; Reprint edition (December, 1995)

[11] C.E. Frouzakis, I.G. Kevrekidis, B. Peckham, *A route to computational chaos revisited: noninvertibility and the breakup of an invariant circle*, Physica D , Vol. 177, 101-121, 2003

[12] A. Katok and B. Hasselblatt, Introduction to the Modern Theorey of Dynamical Systems. Cambridge University Press, 1995.

[13] L. Perko, Differential Equations and Dynamical Systems. Springer-Verlag, 1993.

[14] C. L. Redman, Human Impact on Ancient Environments. University of Arizona Press, Tucson, 1999.

[15] Thompson, J.M.T., . *Non-Linear Dynamics and Chaos.* John Wiley & Sons, Toronto, (1986).

[16] P. Turchin, Complex Population Dynamics: A Theoretical/Empirical Synthesis. Princeton, Princeton, 2003.

[17] Turchin, P. Historical Dynamics: Why States Rise and Fall. Princeton University Press, 2003.